Building and Environment, Volume 68, October 2013, Pages 179-192

CFD evaluation of new second-skin facade concept for wind comfort on building balconies: Case study for the Park Tower in Antwerp

H. Montazeri*, B. Blocken, W.D. Janssen, T. van Hooff

Building Physics and Services, Eindhoven University of Technology, P.O. box 513, 5600 MB Eindhoven, The Netherlands

Graphical abstract

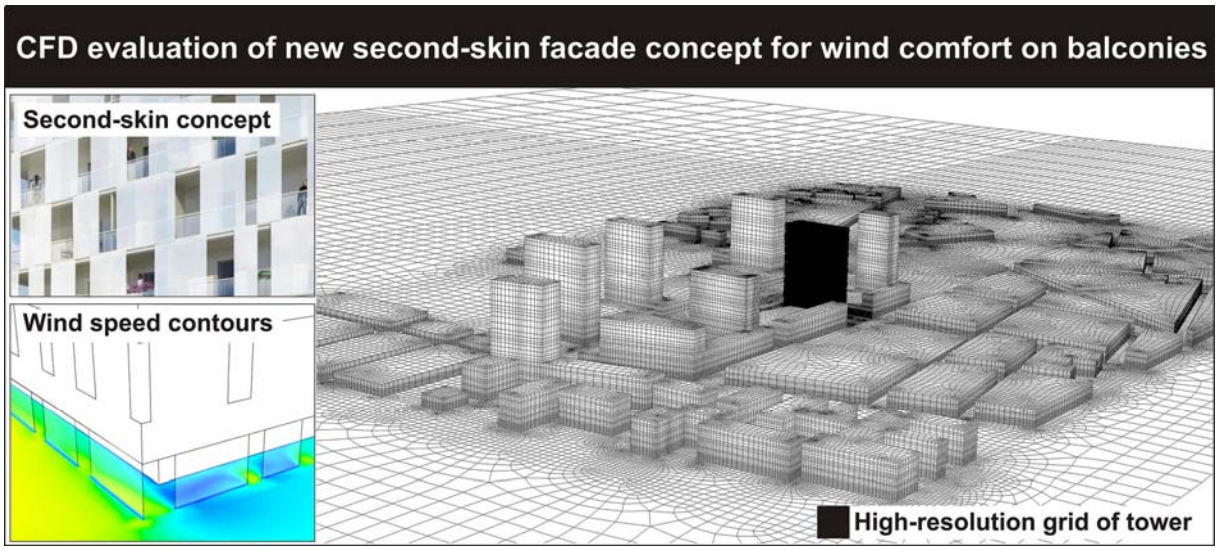

Research highlights:

- High wind speed around high-rise buildings can lead to wind discomfort at building balconies.
- Previous wind comfort studies with CFD focused on ground level around the buildings.
- This paper presents a detailed CFD analysis of wind comfort at balconies of a tower building.
- 3D RANS simulations based on successful validation with wind-tunnel measurements.
- New second-skin facade concept substantially improves wind comfort at balconies.

* **Corresponding author**: Hamid Montazeri, Building Physics and Services, Eindhoven University of Technology, P.O. box 513, 5600 MB Eindhoven, the Netherlands. Tel: +31 (0)40 247 5790, Fax: +31 (0)40 243 8595.
E-mail address: h.montazeri@tue.nl

Building and Environment, Volume 68, October 2013, Pages 179-192

CFD evaluation of new second-skin facade concept for wind comfort on building balconies: Case study for the Park Tower in Antwerp

H. Montazeri*, B. Blocken, W.D. Janssen, T. van Hooff

Building Physics and Services, Eindhoven University of Technology, P.O. box 513, 5600 MB Eindhoven, The Netherlands

Abstract

High wind speed around high-rise buildings can lead to wind discomfort or wind danger at building balconies. This paper presents the evaluation of a new facade concept that is intended to significantly reduce the wind speed and therefore improve wind comfort on the balconies of high-rise buildings. The concept consists of a staggered semi-open second-skin facade in front of the balconies, which partly shields them from the wind. The concept is evaluated for the new 78 m high Park Tower in the urban area of Antwerp, where it will be implemented. 3D steady Reynolds-Averaged Navier-Stokes Computational Fluid Dynamics (CFD) simulations are performed for the case with and without this facade concept. The simulations are made with the realizable k-ε turbulence model on a high-resolution grid. Validation is conducted using wind-tunnel measurements of surface pressure distribution on a building model with balconies. Wind comfort for the Park Tower is assessed with the Dutch wind nuisance standard NEN8100 for the case with and without the second-skin facade concept. The analysis shows that this concept is effective in providing a zone with pressure equalisation at the balconies. The related reduction in pressure gradients across the width of the facade strongly decreases the local wind speed. At many positions along the balconies this yields a wind comfort improvement of one or even two classes in the Dutch wind nuisance standard compared to the situation without implementation of this concept.

Keywords: Wind nuisance and danger; Balcony; Terraces; Urban area; Computational Fluid Dynamics (CFD); Built environment

1. Introduction

Wind comfort and wind safety for pedestrians are important requirements in urban areas [1-12]. Many urban authorities recognize this importance and only grant a permit for a new building after a wind comfort and wind safety assessment study has shown a sufficient degree of comfort and safety. Wind comfort assessment studies consist of combining statistical meteorological data with aerodynamic information and a comfort criterion. The aerodynamic information is needed to transform the statistical meteorological data from the weather station to the location of interest at the building site, after which it is combined with a comfort criterion to judge local wind comfort. The aerodynamic information usually consists of two parts: the terrain-related contribution and the design-related contribution. The terrain-related contribution represents the change in wind statistics from the meteorological site to a reference location near the building site. The design-related contribution represents the change in wind statistics due to the local urban design, i.e. the configuration of the buildings. It can be obtained by either wind-tunnel testing or numerical simulation with Computational Fluid Dynamics (CFD).

CFD offers some specific advantages compared to wind tunnel testing. It does not suffer from scaling problems and similarity constraints, because simulations can be performed at full scale. This can become important when flow at a wide range of relevant length scales needs to be considered, such as flow around facade details such as balconies on a building that is part of a large urban area, as will be the case in this paper. CFD also provides whole-flow field data, i.e. information on the relevant parameters at every position in the model, while wind-tunnel measurements are generally only performed at a limited number of selected positions. However, the reliability and accuracy of CFD are important concerns, and solution verification and validation

* **Corresponding author**: Hamid Montazeri, Building Physics and Services, Eindhoven University of Technology, P.O. box 513, 5600 MB Eindhoven, the Netherlands. Tel: +31 (0)40 247 5790, Fax: +31 (0)40 243 8595.
E-mail address: h.montazeri@tue.nl

studies are imperative. Recently, the use of CFD in wind comfort studies has received strong support from several international initiatives that focused on the establishment of general best practice guidelines (e.g. [6,9,13-17]). Strong support has also been provided by specific guidelines such as those for the validation of simulations of urban wind flow [18,19], the simulation of equilibrium atmospheric boundary layers (e.g. [20-27]) and the generation of high-resolution and high-quality computational grids (e.g. [28,29]).

In the past, several CFD studies of pedestrian-level wind conditions around buildings and/or in complex urban environments have been performed [1-5,7-12,23,30-45]. The majority of these studies were conducted with the 3D steady Reynolds-averaged Navier-Stokes (RANS) approach. Most previous studies on pedestrian-level wind conditions included validation by comparison of the CFD results with wind-tunnel measurements for the same building or urban configuration [3,5,7,8,31-33,36-38,41]. A smaller number of previous studies provided a comparison with field measurements [7,11,44,45]. Other studies applied so-called sub-configuration validation [40,43], which is also the approach that is used in the present paper. Sub-configuration validation refers to performing validation for simpler generic building configurations that represent sub-configurations of the more complex urban configuration. For these generic configurations, wind-tunnel measurements are generally available in the literature. The confidence extracted from this validation study can be used to support the application of CFD with similar computational parameters for the more complex urban configuration.

Although many studies of pedestrian-level wind speed conditions have been performed in the past, they almost exclusively focused on wind speed near ground-level. To the best of our knowledge, only one CFD study has yet been published with focus on wind conditions on building balconies [30]. In this pioneering paper on CFD applications in wind engineering, Murakami [30] numerically assessed the impact of providing a solid partition fence at the corner of a balcony area. Attention for wind conditions and wind comfort at building balconies on high-rise buildings is important, because they can be exposed to strong winds and comfort and safety of the pedestrians at the balconies needs to be ensured. In order to reduce wind discomfort on balconies, different measures can be taken, such as closing the balcony or adding partition walls, as in the study by Murakami [30]. Recently a new facade concept was developed by ELD Partnership, which provides another way of shielding the balcony area from strong winds. It consists of a staggered semi-open second-skin facade that partly shields the balconies from the wind (Fig. 1a-c). The concept is intended to provide a semi-outdoor environment at the balconies, which also includes significant improvement of wind comfort on the building balconies. The concept is implemented in the Park Tower ("Parktoren"), which is a new 78 m high-rise building in the urban area of Antwerp, Flanders, Belgium (Fig. 1d). In this paper, the performance of this concept for this tower is evaluated by CFD simulations based on the 3D steady RANS equations and application of the Dutch wind nuisance standard NEN8100, and by comparing the results for the situation with and without application of this new facade concept. The CFD simulations are subjected to a detailed validation study based on the sub-configuration validation methodology mentioned above.

In section 2, the building and facade geometry and the building surroundings are described. Section 3 presents the CFD validation study. In section 4, the computational settings and parameters for the case study of the Park Tower are outlined. The computational results are presented in section 5, and wind comfort is assessed with the Standard in section 6. Finally, a discussion (section 7) and conclusions (section 8) are provided.

2. Description of building and surroundings

The new high-rise building Park Tower ("Parktoren") is located in Park Spoor Noord in the northern part of the city of Antwerp, Flanders, Belgium. The tower is north-south oriented and surrounded by other high-rise and low-rise buildings (Fig. 1d). It has dimensions L × W × H = 21.87 × 50.88 × 78.18 m³ (Fig. 2). The depth of the balconies on the north, east, south and west side of the tower is 1.32 m, 1.3 m, 1.59 m and 1.56 m, respectively. The facade concept is a second-skin concept, where a second outer skin is placed in front of the first and inner skin. The inner skin acts as traditional facade and the outer skin as a wind shield for the balconies between both skins (Fig. 1, 2). The second skin consists of a staggered semi-open glass facade, as indicated in Figure 1a-c. It has a permanent solid glass balustrade of 1.2 m high, while above this 1.2 m, solid glass facade panels are applied in a staggered configuration. The width of the openings in the second-skin façade ranges from 0.69 to 2.45 m. The porosities of the north, east, west and south facade are 20%, 18%, 20% and 18%, respectively. Note that no partition walls are present in the balcony area, and that this area is completely open for wind flow all along the circumference of the facade. For the comparison study, a reference high-rise building with only the 1.2 m high and non-porous balustrade will be considered. Figure 1d shows a perspective view of some of the surrounding buildings. The buildings in "white" are all part of the new developments in this area. A plan view of the surrounding buildings is shown in Figure 3 on a grid of about 1000 by 630 m². In the immediate vicinity of the Park Tower the high-rise buildings A,B, C and D have a height of 79 m, and building E is 58 m high. Figure 4 shows a plan view of the wider surroundings with a radius of 10 km around the building under study. The computational domain is indicated by the central black rectangle in the figure. This view with indication of the land use is needed to estimate the value of the aerodynamic roughness length z_0 for all 12 wind

direction intervals that will be studied. Given the gradual development of internal boundary layers due to roughness changes, a 10 km fetch is required to determine z_0. This estimate is made for twelve wind direction sectors, based on the updated Davenport roughness classification [46]. These z_0 values are an important parameter in the inlet profiles for the CFD simulations and as a measure for the equivalent sand-grain roughness parameters to be inserted into the wall functions.

3. CFD validation study

CFD simulations based on the 3D steady RANS equations in combination with a turbulence model require validation. As mentioned before, the present study employs "sub-configuration validation". Because the validation study has been published as a separate paper [47], only the headlines are briefly repeated here.

3.1. Wind-tunnel measurements

Atmospheric boundary layer wind-tunnel measurements of wind-induced surface pressure on the facade of a reduced-scale model (1:30) of a medium-rise building were reported by Chand et al. [48]. The incident vertical profile of mean wind speed (i.e. at the location of the model at the turntable) can be described by a logarithmic law with aerodynamic roughness length z_0 = 0.008 m and friction velocity u* = 0.72 m/s. Longitudinal turbulence intensity ranged from 13% near ground level to about 3% at gradient height. The building had dimensions $w_m \times d_m \times h_m = 0.25 \times 0.60 \times 0.50$ m^3 (reduced scale, see Fig. 5a) corresponding to full-scale dimensions $W_m \times D_m \times H_m = 7.5 \times 18 \times 15$ m^3. Three balconies were positioned at each floor. Each balcony has length 0.15 m, width 0.05 m and height 0.03 m (reduced scale) corresponding to full-scale dimensions 4.5 m, 1.5 m and 0.9 m, respectively. Surface pressures were measured along three vertical lines on the windward and leeward facade. Each line was positioned at the middle of the balconies and 45 pressure taps were implemented along these lines. Pressure coefficients C_p were related to the incident wind speed at building height (U_{ref} = 7.1 m/s).

3.2. CFD simulations: computational settings and parameters

A computational model was made of the reduced-scale building model used in the wind-tunnel measurements. The CFD simulations were performed following the best practice guidelines by Franke et al. [6,14] and Tominaga et al. [9]. The size of the computational domain was chosen according to [6,9,14].The computational grid was created using the surface-grid extrusion technique [29]. The grid resolution resulted from a grid-sensitivity analysis, yielding a hybrid grid with 2,102,250 prismatic and hexahedral cells. Part of the grid is shown in Figure 5b. A total number of 20 and 10 cells were used along the width and depth of the balconies, respectively. More information about the grid can be found in [47]. The inlet boundary conditions (mean wind speed U, turbulent kinetic energy k and turbulence dissipation rate ε) were based on the measured incident vertical profiles of mean wind speed U and longitudinal turbulence intensity I_u. The commercial CFD code Fluent 6.3.26 was used to perform the simulations. The 3D steady RANS equations were solved in combination with the realizable k−ε turbulence model by Shih et al. [49]. The SIMPLE algorithm was used for pressure-velocity coupling, pressure interpolation was second order and second-order discretization schemes were used for both the convection terms and the viscous terms of the governing equations. More information about solver settings is given in [47]. Convergence was obtained when all the scaled residuals levelled off and reached a minimum of 10^{-6} for x, y momentum, 10^{-5} for z momentum and 10^{-4} for k, ε and continuity.

3.3. Comparison between CFD simulations and wind-tunnel measurements

The CFD results are compared with the wind-tunnel measurements in terms of the pressure coefficient:

$$C_P = \frac{P - P_0}{0.5 \rho U_{ref}^2} \quad (1)$$

where P is the pressure at the surface, P_0 the reference static pressure, ρ = 1.225 kg/m³ the air density and U_{ref} the reference wind speed at building height (U_{ref} = 7.1 m/s at z = 0.5 m). Figures 6a-b compare the numerically simulated and measured C_p at the windward facade for wind direction 0°, showing a very close agreement, with average absolute deviations of 0.052 and 0.072, respectively, which corresponds to relative deviations of 14% and 11%. Figures 6c-d provide the same comparison for the leeward facade. The average absolute deviations are 0.069 and 0.070, respectively, which corresponds to relative deviations of 14% and 15%. Especially for the leeward facade, the fairly good agreement between simulations and measurements is remarkable, because it is known that steady RANS CFD is generally deficient in reproducing the wind-flow pattern downstream of windward facades [42,50]. Nevertheless, the deviation is still significant, and it indicates that the numerically

predicted back pressure level shows a higher recovery compared to the experimental results. This is attributed to the weaker wake structure behind the building in the CFD simulations. This is a deficiency of steady RANS modelling, as outlined in [42,50]. Regardless of the origin of this deviation, it is important to note that in the present paper the focus is on the wind speed at the windward facades rather than at the leeward facades. At first sight, this might seem strange in the framework of a wind comfort study that uses wind statistics in which all wind directions are represented. However, the focus on wind speed at the windward facades is justified, because in wind comfort studies the positions with high wind speed are important, i.e. positions where a certain threshold wind speed is exceeded. The other positions, such as leeward balconies, are therefore less important. The reason is that the wind speed will be much lower there and will therefore not contribute substantially to the wind comfort exceedance probability, as outlined by Blocken et al. [11] and Janssen et al. [45]. Figure 7 shows that also for oblique incident wind (45°), CFD simulations and wind-tunnel measurements show a good agreement for the windward facade. The average absolute deviations in Figure 7a-c are 0.028, 0.029 and 0.028, respectively. The conclusion from the validation study is that the 3D steady RANS equations in combination with the realizable k-ε model, high-resolution grid, standard wall functions and second-order discretisation schemes can provide a satisfactory representation of wind pressure at the windward facade of a building with balconies. Therefore, the same approach with the same turbulence models, wall functions, discretisation schemes and a similar computational grid will be used in the case study. Note that a validation study based on surface pressures across the facade is considered appropriate here because these pressures drive the near-wall wind flow at the balconies across this facade.

4. CFD simulations for the case study: computational settings and parameters

4.1. Computational geometry and domain

The Park Tower and its urban surroundings are placed in a computational domain with dimensions $W_d \times D_d \times H_d = 2076 \times 1963 \times 400$ m^3. This actual computational domain consists of a subdomain containing the explicitly modelled buildings (i.e. those included in the computational domain with their actual main dimensions) and an additional downstream subdomain, as shown in Figure 8. The explicitly modelled buildings are the tower itself and the surrounding buildings in a rectangle of 1037 by 632 m² around the tower. The tower is modelled in detail, including second-skin facade with the details of the staggered facade elements as shown in Figure 2, while the surrounding buildings are included only with their main shape. Special attention is given to the generation of a high-quality and high-resolution grid. The grid is constructed using the surface-grid extrusion technique presented by van Hooff and Blocken [29], which allows a large degree of control over the quality of the grid and its individual cells. It consists of only hexahedral and prismatic cells and does not contain any tetrahedral or pyramid cells. This technique was used successfully in previous studies for a wide range of applications [11,29,44,45,51-55]. The grid resolution at the building balconies is based on the one used in the validation study, with at least 10 cells across the depth of the balconies. A typical cell size at the balconies is 0.1 m. The resulting grid has a total of 16,292,495 hexahedral and prismatic cells. The computational geometry and grid are depicted in Figure 9 and 10. For comparison purposes, a similar computational domain and grid are made for the Park Tower without second-skin facade. This grid consists of 15,536,529 hexahedral and prismatic cells (Fig. 10 c-d).

4.2. Boundary conditions and solver settings

At the inlet of the domain, neutral atmospheric boundary layer inflow profiles of mean wind speed U (m/s), turbulent kinetic energy k (m²/s²) and turbulence dissipation rate ε (m²/s³) are imposed (Eqs. (2-4). These profiles are based on the aerodynamic roughness length z_0 of the upstream terrain that is not included in the computational domain. Figure 4 shows this terrain and the estimated values of z_0 for different approach-flow wind directions. In Eq. (2) and (4), κ is the von Karman constant (= 0.42). For $z_0 = 0.25$ m, $z_0 = 0.5$ m and $z_0 = 1$ m the inlet longitudinal turbulence intensity (I_u) ranges from 22%, 29% and 39% at pedestrian height (z = 1.75 m) to 3%, 5% and 8% at gradient height, respectively. The corresponding values of u^*_{ABL}, for a reference wind speed at 10 m height of 5 m/s, are 0.54, 0.66 and 0.83 m/s. The turbulent kinetic energy k is calculated from U and I_u using Eq. (3) and assuming that the standard deviations of the turbulent fluctuations in the three directions are similar ($\sigma_u = \sigma_v = \sigma_w$).

$$U(z) = \frac{u^*_{ABL}}{\kappa} \ln\left(\frac{z + z_0}{z_0}\right) \tag{2}$$

$$k(z) = 1.5\left(I_U(z)U(z)\right)^2 \tag{3}$$

$$\varepsilon(z) = \frac{u_{ABL}^{*3}}{\kappa(z + z_0)} \tag{4}$$

For the ground surface, the standard wall functions by Launder and Spalding [56] with roughness modification by Cebeci and Bradshaw [57] are used. The values of the roughness parameters, i.e. the sand-grain roughness height k_s (m) and the roughness constant C_s, are determined using their consistency relationship with the aerodynamic roughness length z_0 derived by Blocken et al. [21]. For Fluent 6.3, this relationship is:

$$k_s = \frac{9.793 z_0}{C_s} \tag{5}$$

Standard wall functions are also used at the building surfaces, but with zero roughness height $k_s = 0$ ($C_s = 0.5$). Zero static pressure is applied at the outlet plane. Symmetry conditions, i.e. zero normal velocity and zero normal gradients of all variables, are applied at the top and lateral sides of the domain.

The solver settings are identical to those in the validation study reported in section 3. The 3D steady RANS equations with the realizable k-ε turbulence model are solved for the 12 wind directions θ = 0-330° in 30° intervals. Convergence is obtained when the scaled residuals showed no further reduction with increasing number of iterations and at that time the residuals reached the following minimum values; x-, y- and z-momentum: 10^{-7}, k and ε: 10^{-6} and continuity: 10^{-5}.

5. CFD simulations for the case study: results

Figure 11 shows a perspective view of contours of the amplification factor in horizontal planes at different heights. The amplification factor is defined as the ratio between the local mean wind speed and the "undisturbed" mean wind speed at the same height, i.e. the wind speed that would occur without the buildings present. The amplification factor is therefore a direct indication of the influence of the buildings on the local wind-flow pattern. The planes are taken at the 15th, 10th and 5th floor, at 1.7 m above the balcony floors. The wind direction is 210°, which is the prevailing wind direction in Antwerp. Figure 11a, c and e show the results for the case of the tower with second-skin facade concept, while Figure 11b, d and f show the results for the reference case. Especially for the long west facade, clearly a substantial reduction of the amplification factor is achieved at the balconies behind the second-skin facade.

To analyse this in more detail, Figure 12 provides a top view of the same horizontal cross-sections and for the same wind direction. By comparing the results with and without the second-skin concept, the following observations are made, which apply at every floor:

(1) At the west (windward) facade, the second-skin concept provides a more uniform and also lower value of the amplification factor.
(2) At the south (windward) facade, the amplification factor does not become more uniform, but overall it is reduced.
(3) At the north and east (leeward) facades, the second-skin concept increases the amplification factor.
(4) Overall, the second-skin facade seems to provide a more uniform amplification factor over the entire balcony area, i.e. the whole circumference of the building. An exception to this are the north-west and south-east corner, where pressure short-circuiting between windward and leeward facade parts very locally yields a local amplification factor of about 1. It should be noted that no partition walls are present in the balcony area, and that this area is completely open for wind flow all along the circumference of the facade.

Figure 13 displays contours of the pressure coefficient $C_p = (P-P_0)/(0.5\rho U_{ref}^2)$ in the same horizontal planes as in Figure 12. Note that P is the static air pressure. The figures show that the second-skin facade acts as a semi-permeable barrier that provides some degree of pressure equalisation at the balcony area between the two facade layers. While Figure 13b shows large pressure gradients along the south facade wall, in Figure 13a the second-skin facade shifts those gradients away from the balconies to the outside of the second facade. Similar observations are made for the other floors and – to a lesser extent – for the west facade. The reduction of these pressure gradients along the south and west facades leads to lower wind speed and lower amplification factors along these facades. Conversely, the second-skin facade increases the pressure gradients at the balconies at the leeward facades, which explains the increased amplification factors at these balconies.

Similar results are obtained for the other wind directions, although somewhat less pronounced, because of the shielding effect by surrounding buildings that is present for many of the other wind directions, as can be seen in Figure 1d.

The effect of the second-skin facade concept on mean wind speed can be indicated more clearly by Figure 14, which shows contours of the ratio of mean wind speed without second-skin facade concept and mean wind speed with this concept, in a horizontal plane at a height of 1.7 m above balcony level for wind directions 210° and 90°, and for three floors: 15th, 10th and 5th floor. Note that the higher this ratio, the more effective the shielding effect

by the second-skin facade concept. However, for a complete indication of the effectiveness of the second-skin facade concept, Figure 14 should be combined with Figure 12, because in terms of wind comfort, reductions in mean wind speed will be more effective at those positions where the amplification factors are the highest.

6. Assessment of wind comfort

Wind comfort assessment in this case study is performed with the Dutch standard for wind comfort and wind safety [58,59]. This standard was developed based on extensive research work by Verkaik [60,61], Willemsen and Wisse [62,63], Wisse and Willemsen [64], Wisse et al. [65], and others. It contains an improved and verified transformation model for the terrain-related contribution (see section 1) that can provide the wind statistics at every location in the Netherlands, however without including the local building aerodynamic effects, which are part of the so-called design related contribution and which were presented in section 5 of this paper. Although thermal comfort is also important [5,66], wind comfort and safety generally only refer to the mechanical effects of wind on people [1,63,67]. In the standard, the comfort criterion has a threshold of the mean wind speed U_{THR} = 5 m/s for all types of activities. Depending on the type of activity and the maximum allowed discomfort probability, the code defines fives grades of wind comfort A–E (see Table 1). Although the standard does not specify requirements for balconies, one could assume that class A or B are required, which implies P < 5% and a good or moderate comfort for sitting. To determine the exceedance probability, three steps have to be taken for each of the 12 wind directions.

(1) Obtain wind speed ratios ($\gamma = U/U_{ref,60m}$) from the CFD simulations. The reference wind speed value ($U_{ref,60m}$) is the value of the inlet mean wind speed profile at a height of 60 m. Note that this wind speed ratio differs from the amplification factor that was used to present the results in the previous section;
(2) Convert threshold wind speed at pedestrian level to a threshold wind speed at a height of 60 m ($U_{THR,60m} = U_{THR}/\gamma$);
(3) Determine the percentage of time that the threshold value for the hourly mean wind speed at 60 m is exceeded according to the wind statistics. For the present study, the wind statistics of Eindhoven are used, given its proximity to Antwerp and the absence of statistical meteorological data for Antwerp. The wind statistics for the 12 wind directions for Eindhoven are provided by the Dutch Practice Guideline NPR 6097. The wind statistics are displayed in Figure 15. The wind rose clearly shows that south-west is the prevailing wind direction, and that this is even more pronounced for high wind speed (Fig. 15b).

The total discomfort probability is the sum of the probabilities for the 12 wind directions. Figure 16 shows these discomfort probabilities for the 5th, 10th and 15th floor. The dominance of the south-west wind direction is reflected by the similarity between Figure 12 and 16. By comparing the results with and without the second-skin concept, the following observations are made:

(1) At the west (windward) facade, the second-skin concept substantially reduces the exceedance probabilities. The size of the reductions is very location dependent, but at many positions it exceeds a factor 2.
(2) At the south (windward) facade, also significant reductions are observed, which are most pronounced for the highest (15th) floor.
(3) At the north and east (leeward) facades, the second-skin concept increases the exceedance probability. This is also most pronounced for the highest floor.

Finally, Figure 17 labels the balconies according to the five quality classes in Table 1 of the Standard. For sitting, class A is good and class B is moderate, while classes C-E are considered to represent a poor wind comfort for this activity. The figure shows that the second-skin facade concept substantially improves the wind comfort on the balconies on the west and south facade, and that this improvement is most pronounced for the highest floors. At most positions, the wind comfort improves with one class, and at some positions even with two classes. On the other hand, the concept causes some decrease in wind comfort on the balconies at the leeward facade. This is for example clear at the east facade at the 15th floor, where the wind comfort at a large part of the balconies shifts from class A to class B.

7. Discussion

In the validation study, relative deviations for the windward facade for wind direction 0° were 12%, while the relative deviations for the leeward facade were 15%. The latter fairly large deviations could incite some concern about the accuracy of steady RANS with the realizable k-e model for wind comfort studies at building balconies. However, it is important to stress that in the present paper the focus is on the wind speed at the windward facades rather than at the leeward facades. At first sight, this might seem strange in the framework of a wind comfort study that uses wind statistics in which all wind directions are represented. However, the focus on wind speed at the windward facades is justified, because in wind comfort studies the positions with high wind speed are important, i.e. positions where a certain threshold wind speed is exceeded. The other positions, such as leeward

balconies, are therefore less important. The reason is that the wind speed will be much lower there and will therefore not contribute substantially to the wind comfort exceedance probability, as outlined by Blocken et al. [11] and Janssen et al. [45].

Some important limitations of this study are mentioned.

- The 3D steady RANS equations have been solved with the realizable k-ε model. It is important to note that steady RANS CFD is generally deficient in reproducing the wind-flow pattern downstream of windward facades [30,42]. Nevertheless, this approach is used in this paper, because the accuracy of the wind-flow pattern at side and the leeward facades is less important in wind comfort studies. The reason is that wind comfort studies typically focus on high wind speed positions, i.e. where a certain threshold wind speed is (5 m/s in the present study) is exceeded. Other positions do not contribute significantly to the exceedance probabilities, as explained earlier in [11,45].
- The validation study focused on mean wind pressure coefficients on the building facade. In terms of wind conditions and wind comfort, a validation study focused on mean wind speed would have been more powerful. Unfortunately, high-quality experimental data on mean wind speed on balconies could not be found in the literature. Therefore, this study has limited itself to validation based on mean wind pressure coefficients.
- No grid-sensitivity analysis was performed. However, special attention was paid to generating a high-resolution and high-quality computational grid. The grid was made using the surface-grid extrusion technique [29] and taking into account best practice guidelines for grid generation [6,9,13,28]. In addition, the grid resolution has been taken either similar or higher than in previous studies for which grid-sensitivity analyses were performed [11,28,45].
- Although thermal comfort is also important [5,66], wind comfort and safety generally only refer to the mechanical effects of wind on people [1,63,67].
- The study has been performed for the wind statistics of Eindhoven, which are also representative for the nearby city of Antwerp.
- The comfort criterion in the Dutch wind nuisance standard is based on a threshold mean wind speed of 5 m/s. It does not explicitly consider turbulent fluctuations. This is in line with the application of the 3D steady RANS approach, which only solves the mean flow field. Nevertheless, future research should focus on Large Eddy Simulation (LES) to further evaluate the second-skin facade concept, especially concerning its effect on gustiness.

Two potential important limitations of the second-skin facade concept, that require further investigation, need to be mentioned:

1) The air flow that can be induced in the balcony area, due to the absence of partition walls (perpendicular to the façade) that would provide a compartmentalisation of the balcony area.
2) The aerodynamically generated noise that could be a result of vortex shedding at the edges of the glass panels.

A more traditional approach of improving wind comfort on building balconies is the provision of partition walls or separating screens – often also applied for privacy reasons - that are perpendicular to the facade. Future work on the second-skin facade concept will evaluate the further improvements that can be achieved by combining this concept with separating screens.

8. Conclusions

High wind speed around high-rise buildings can lead to wind discomfort or wind danger at building balconies. This paper has presented the evaluation of a new facade concept that is intended to significantly reduce the wind speed and therefore improve wind comfort on the balconies of high-rise buildings. The concept consists of a staggered semi-open second-skin facade in front of the balconies, which partly shields them from the wind. The concept is implemented in the Park Tower (“Parktoren”), which is a new 78 m high-rise building in the urban area of Antwerp, Flanders, Belgium. In this paper, the performance of this concept for this tower has been evaluated by CFD simulations based on the 3D steady RANS equations and application of the Dutch wind nuisance standard NEN8100, and by comparing the results for the situation with and without application of this new facade concept. The CFD simulations have been subjected to a detailed validation study based on the sub-configuration validation methodology. Sub-configuration validation refers to performing validation for simpler generic building configurations that represent sub-configurations of the more complex urban configuration. For these generic configurations, wind-tunnel measurements are generally available in the literature. The confidence extracted from this validation study can be used to support the application of CFD with similar computational parameters for the more complex urban configuration. The analysis has shown that the second-skin facade concept is effective in providing a zone with pressure equalisation at the balconies. The related reduction in pressure gradients across the width of the facade strongly decreases the local wind speed. At many positions

along the balconies this yields a wind comfort improvement of one or even two classes in the Dutch wind nuisance standard compared to the situation without implementation of this concept. Future research will consist of a further evaluation of the second-skin facade concept with Large Eddy Simulation and on additional improvement of the wind comfort on building balconies by combining this concept with separating screens.

Acknowledgements

The authors thank ELD Partnership, the designers of the Park Tower and the second-skin facade concept, for the permission to reproduce the figures in Figure 1 and 2. Hardware support for the numerical simulations in this paper was provided by the laboratory of the Unit Building Physics and Services (BPS) of Eindhoven University of Technology. Their support is gratefully acknowledged.

References

[1] Bottema M. Wind climate and urban geometry. PhD thesis, Eindhoven University of Technology, 1993, 212pp.
[2] Mochida A, Tominaga Y, Murakami S, Yoshie R, Ishihara T, Ooka R. Comparison of various k–ε models and DSM applied to flow around a high-rise building—report on AIJ cooperative project for CFD prediction of wind environment. Wind Struct 2002;5:227–44.
[3] Richards PJ, Mallinson GD, McMillan D, Li YF. Pedestrian level wind speeds in downtown Auckland. Wind Struct 2002;5:151-64.
[4] Blocken B, Carmeliet J. Pedestrian wind environment around buildings: Literature review and practical examples. Journal of Thermal Envelope and Building Science 2004;28:107-59.
[5] Stathopoulos T. Pedestrian level winds and outdoor human comfort. J Wind Eng Ind Aerodyn 2006;94:769-80.
[6] Franke J, Hellsten A, Schlünzen H, Carissimo B. Best practice guideline for the CFD simulation of flows in the urban environment. Brussels: COST Office; 2007.
[7] Yoshie R, Mochida A, Tominaga Y, Kataoka H, Harimoto K, Nozu T, Shirasawa T. Cooperative project for CFD prediction of pedestrian wind environment in the Architectural Institute of Japan. J Wind Eng Ind Aerodyn 2007;95:1551-78.
[8] Mochida A, Lun IYF. Pedestrian wind environment and thermal comfort at pedestrian level in urban area. J Wind Eng Ind Aerodyn 2008;96:1498-1527.
[9] Tominaga Y, Mochida A, Yoshie R, Kataoka H, Nozu T, Yoshikawa M, et al. AIJ guidelines for practical applications of CFD to pedestrian wind environment around buildings. J Wind Eng Ind Aerodyn 2008;96:1749-61.
[10] Blocken B, Stathopoulos T, Carmeliet J, Hensen JLM. Application of CFD in building performance simulation for the outdoor environment: an overview. J Building Perform Simul 2011;4(2):157-84.
[11] Blocken B, Janssen WD, van Hooff T. CFD simulation for pedestrian wind comfort and wind safety in urban areas: General decision framework and case study for the Eindhoven University campus. Environ Modell Softw 2012;30:15-34.
[12] Moonen P, Defraeye T, Dorer V, Blocken B, Carmeliet J. Urban physics: effect of the microclimate on comfort, health and energy demand. Frontiers of Architectural Research 2012;1:197-228.
[13] Casey M, Wintergerste, T. Best Practice Guidelines, ERCOFTAC Special Interest Group on Quality and Trust in Industrial CFD, ERCOFTAC, Brussels. 2000.
[14] Franke J, Hirsch C, Jensen AG, Krüs HW, Schatzmann M, Westbury PS, Miles SD, Wisse JA, Wright NG. Recommendations on the use of CFD in wind engineering. Proc. Int. Conf. Urban Wind Engineering and Building Aerodynamics, (Ed. van Beeck JPAJ), COST Action C14, Impact of Wind and Storm on City Life Built Environment, von Karman Institute, Sint-Genesius-Rode, Belgium: 2004.
[15] Jakeman AJ, Letcher RA, Norton JP. Ten iterative steps in development and evaluation of environmental models. Environ Modell Softw 2006;21:602-14.
[16] Britter R, Schatzmann M. (Eds.). Model Evaluation Guidance and Protocol Document COST Action 732. COST Office Brussels, ISBN 3-00-018312-4. 2007.
[17] Blocken B, Gualtieri C. Ten iterative steps for model development and evaluation applied to Computational Fluid Dynamics for Environmental Fluid Mechanics. Environ Modell Softw 2012;33:1-22.
[18] Schatzmann M, Rafailidis S, Pavageau M. Some remarks on the validation of small-scale dispersion models with field and laboratory data. J Wind Eng Ind Aerodyn 1997;67-68:885-93.
[19] Schatzmann M, Leitl B. Issues with validation of urban flow and dispersion CFD models. J Wind Eng Ind Aerodyn 2011;99(4):169-86.
[20] Richards PJ, Hoxey RP. Appropriate boundary conditions for computational wind engineering models using the k-ε turbulence model. J Wind Eng Ind Aerodyn 1993;46&47:145-53.

[21] Blocken B, Stathopoulos T, Carmeliet J. CFD simulation of the atmospheric boundary layer: wall function problems. Atmos Environ 2007;41:238-52.
[22] Hargreaves DM, Wright NG, On the use of the k–ε model in commercial CFD software to model the neutral atmospheric boundary layer. J Wind Eng Ind Aerodyn 2007;95:355-69.
[23] Blocken B, Carmeliet J, Stathopoulos T. CFD evaluation of wind speed conditions in passages between parallel buildings—effect of wall-function roughness modifications for the atmospheric boundary layer flow. J Wind Eng Ind Aerodyn 2007;95:941-62.
[24] Yang Y, Gu M, Chen S, Jin X. New inflow boundary conditions for modelling the neutral equilibrium atmospheric boundary layer in computational wind engineering. J Wind Eng Ind Aerodyn 2009;97:88-95.
[25] Gorlé C, van Beeck J, Rambaud P, Van Tendeloo G. CFD modelling of small particle dispersion: the influence of the turbulence kinetic energy in the atmospheric boundary layer. Atmos Environ 2009;43:673-81.
[26] Richards PJ, Norris SE. Appropriate boundary conditions for computational wind engineering models revisited. J Wind Eng Ind Aerodyn 2011;99:257-66.
[27] Parente A, Gorlé C, van Beeck J, Benocci C. Improved k–ε model and wall function formulation for the RANS simulation of ABL flows. J Wind Eng Ind Aerodyn 2011;99:267-78.
[28] Tucker PG, Mosquera A. NAFEMS introduction to grid and mesh generation for CFD. NAFEMS CFD Working Group, R0079. 2001, 56 pp.
[29] van Hooff T, Blocken B. Coupled urban wind flow and indoor natural ventilation modelling on a high-resolution grid: A case study for the Amsterdam ArenA stadium. Environ Modell Softw 2010;25:51-65.
[30] Murakami S. Computational wind engineering. J Wind Eng Ind Aerodyn 1990;36:517-38.
[31] Gadilhe A, Janvier L, Barnaud G. Numerical and experimental modelling of the three-dimensional turbulent wind flow through an urban square. J Wind Eng Ind Aerodyn 1993;46-47:755-63.
[32] Takakura S, Suyama Y, Aoyama M. Numerical simulation of flowfield around buildings in an urban area. J Wind Eng Ind Aerodyn 1993;46-47:765-71.
[33] Stathopoulos T, Baskaran A. Computer simulation of wind environmental conditions around buildings. Eng Struct 1996;18:876–85.
[34] Baskaran A, Kashef A. Investigation of air flow around buildings using computational fluid dynamics techniques. Eng Struct 1996;18:861-73.
[35] He J, Song CCS. Evaluation of pedestrian winds in urban area by numerical approach. J Wind Eng Ind Aerodyn 1999;81:295-309.
[36] Ferreira AD, Sousa ACM, Viegas DX. Prediction of building interference effects on pedestrian level comfort. J Wind Eng Ind Aerodyn 2002;90:305–19.
[37] Miles SD, Westbury PS. Assessing CFD as a tool for practical wind engineering applications. Proc. Fifth UK Conf. Wind Engineering, 2002.
[38] Westbury PS, Miles SD, Stathopoulos T. CFD application on the evaluation of pedestrian-level winds. Workshop on Impact of Wind and Storm on City Life and Built Environment, Cost Action C14, CSTB, June 3–4, Nantes, France: 2002.
[39] Hirsch C, Bouffioux V, Wilquem F. CFD simulation of the impact of new buildings on wind comfort in an urban area. Workshop Proceedings, Cost Action C14, Impact of Wind and Storm on City Life and Built Environment. Nantes, France: 2002.
[40] Blocken B, Roels S, Carmeliet J. Modification of pedestrian wind comfort in the Silvertop Tower passages by an automatic control system. J Wind Eng Ind Aerodyn 2004;92:849-73.
[41] Blocken B, Moonen P, Stathopoulos T, Carmeliet J. Numerical study on the existence of the venturi effect in passages between perpendicular buildings. J Eng Mech - ASCE 2008;134:1021-8.
[42] Tominaga Y, Mochida A, Murakami S, Sawaki S. Comparison of various revised k–ε models and LES applied to flow around a high-rise building model with 1:1:2 shape placed within the surface boundary layer. J Wind Eng Ind Aerodyn 2008;96:389-411.
[43] Blocken B, Carmeliet J. Pedestrian wind conditions at outdoor platforms in a high-rise apartment building: generic sub-configuration validation, wind comfort assessment and uncertainty issues, Wind Struct 2008;11:51-70.
[44] Blocken B, Persoon J. Pedestrian wind comfort around a large football stadium in an urban environment: CFD simulation, validation and application of the new Dutch wind nuisance standard. J Wind Eng Ind Aerodyn 2009;97:255-70.
[45] Janssen WD, Blocken B, van Hooff T. Pedestrian wind comfort around buildings: Comparison of wind comfort criteria based on whole-flow field data for a complex case study. Build Environ 59:547-62.
[46] Wieringa J. Updating the Davenport roughness classification. J Wind Eng Ind Aerodyn 1992;41-44:357-68.
[47] Montazeri H, Blocken B. CFD simulation of wind-induced pressure coefficients on buildings with and without balconies: Validation and sensitivity analysis. Build Environ 2013;60:137-49.

[48] Chand I, Bhargava PK, Krishak NLV. Effect of balconies on ventilation inducing aeromotive force on low-rise buildings. Build Environ 1998;33:385-96.
[49] Shih T-H, Liou WW, Shabbir A, Yang Z, Zhu J. A new k-ϵ eddy viscosity model for high reynolds number turbulent flows. Comput Fluids 1995;24:227-38.
[50] Murakami S. Comparison of various turbulence models applied to a bluff body. J Wind Eng Ind Aerodyn 1993;46–47:21-36.
[51] van Hooff T, Blocken B. On the effect of wind direction and urban surroundings on natural ventilation of a large semi-enclosed stadium. Comput Fluids 2010;39:1146-55.
[52] van Hooff T, Blocken B, van Harten M. 3D CFD simulations of wind flow and wind-driven rain shelter in sports stadia: influence of stadium geometry. Build Environ 2011;46(1):22-37.
[53] van Hooff T, Blocken B, Aanen L, Bronsema B. A venturi-shaped roof for wind-induced natural ventilation of buildings: wind tunnel and CFD evaluation of different design configurations. Build Environ 2011;46:1797-807.
[54] Gousseau P, Blocken B, Stathopoulos T, van Heijst GJF. CFD simulation of near-field pollutant dispersion on a high-resolution grid: a case study by LES and RANS for a building group in downtown Montreal. Atmos Environ 2011;45:428-38.
[55] Ramponi R, Blocken B. CFD simulation of cross-ventilation for a generic isolated building: impact of computational parameters. Build Environ 2012;53:34-48.
[56] Launder BE, Spalding DB. The numerical computation of turbulent flows. Comput Methods Appl Mech Eng 1974;3:269–89.
[57] Cebeci T, Bradshaw P. Momentum transfer in boundary layers. New York: Hemisphere Publishing Corp; 1977.
[58] NEN 2006. Wind comfort and wind danger in the built environment, NEN 8100 (in Dutch) Dutch Standard.
[59] NEN 2006. Application of mean hourly wind speed statistics for the Netherlands, NPR 6097:2006 (in Dutch). Dutch Practice Guideline.
[60] Verkaik JW. Evaluation of two gustiness models for exposure correction calculations. J Appl Meteorol 2000;39:1613-26.
[61] Verkaik JW. On wind and roughness over land. PhD thesis. Wageningen University. The Netherlands, 2006, 123 pp.
[62] Willemsen E, Wisse JA. Accuracy of assessment of wind speed in the built environment. J Wind Eng Ind Aerodyn 2002;90:1183-90.
[63] Willemsen E, Wisse JA,. Design for wind comfort in The Netherlands: Procedures, criteria and open research issues. J Wind Eng Ind Aerodyn 2007;95:1541-50.
[64] Wisse JA, Willemsen E. Standardization of wind comfort evaluation in the Netherlands. 11th Int Conf Wind Eng (11ICWE), Lubbock, Texas: 2003.
[65] Wisse JA, Verkaik JW, Willemsen E. Climatology aspects of a wind comfort code, 12th Int Conf Wind Eng (12ICWE), Cairns, Australia: 2007.
[66] Metje N, Sterling M, Baker CJ. Pedestrian comfort using clothing values and body temperatures. J Wind Eng Ind Aerodyn 2008;96:412-35.
[67] Lawson TV, Penwarden AD,. The effects of wind on people in the vicinity of buildings, Proceedings 4th International Conference on Wind Effects on Buildings and Structures, Cambridge University Press, Heathrow: 1975. p. 605–622.

FIGURES

Figure 1. (a) Building facade with second-skin staggered facade concept. (b) Bottom of Park Tower with the second-skin concept, view from south-east. (c) Full view from south. (d) View of Park Tower (red), other new buildings under development (white) and already existing urban surroundings at the time of writing this paper.

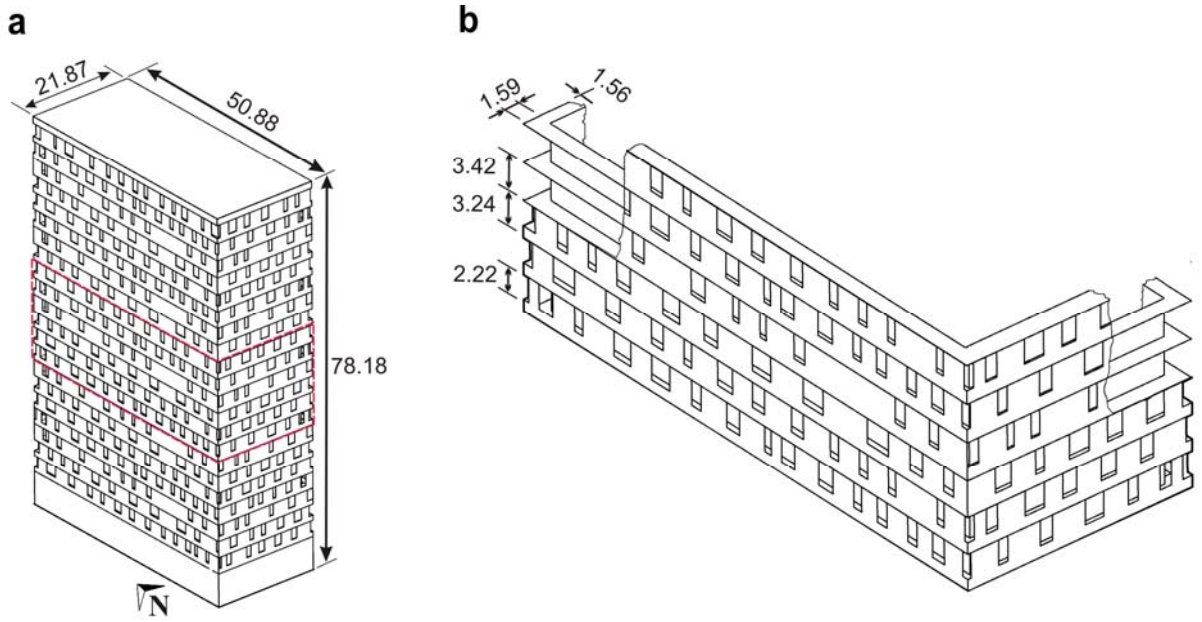

Figure 2. (a,b) Geometry of Park Tower and of part of second-skin facade. Dimensions in meter.

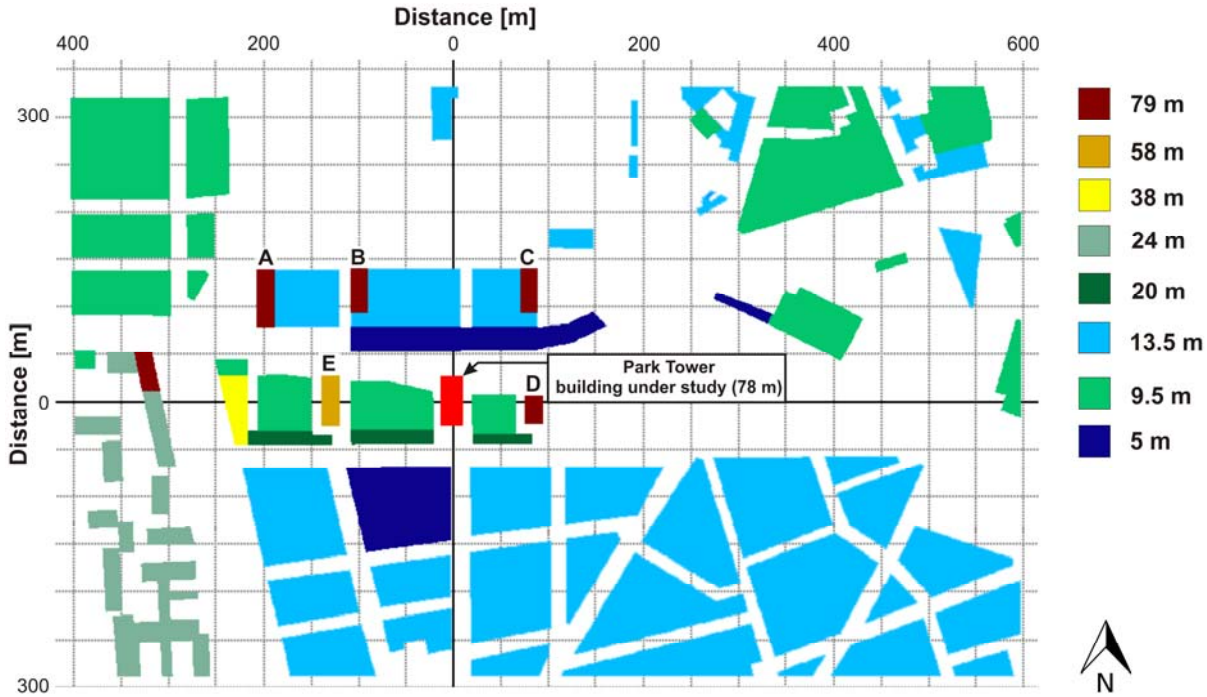

Figure 3. Top view of Park Tower and wider surroundings in a rectangular area of 630 to 1000 m^2 with indication of building heights. Dimensions in meter.

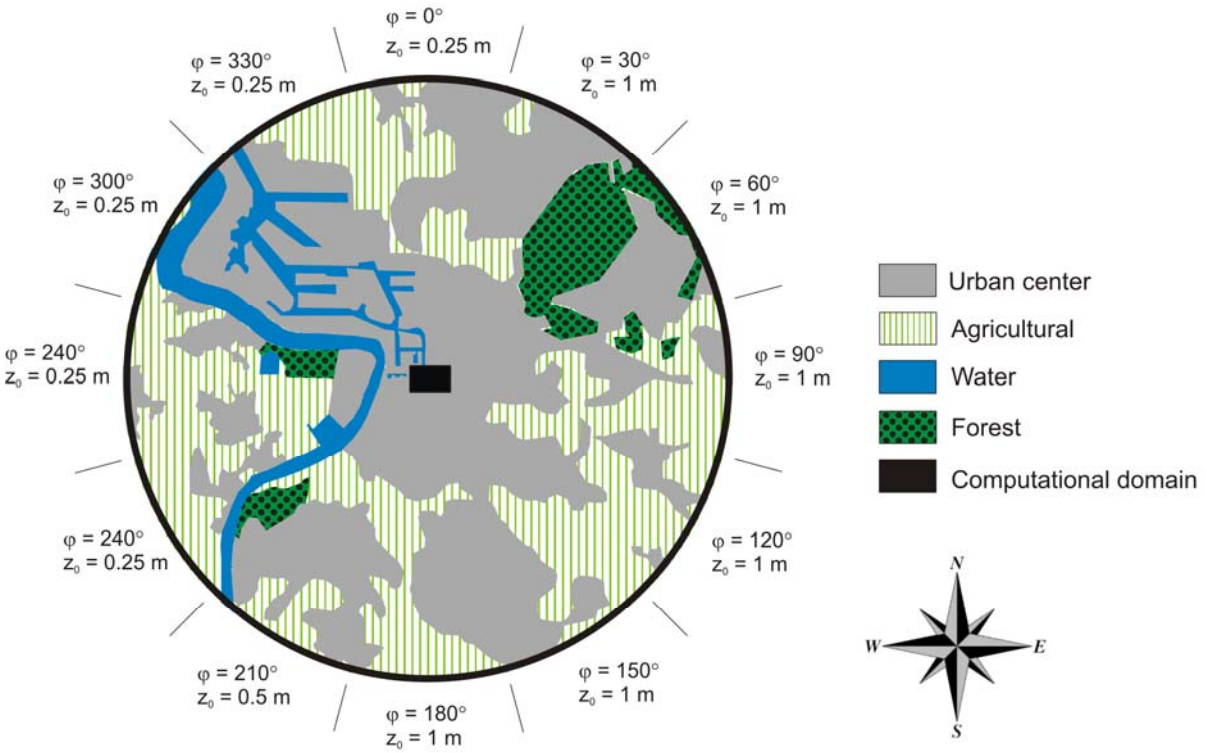

Figure 4. Surroundings of Park Tower in a 10 km radius with associated aerodynamic roughness length z_0. The computational domain used in this study is indicated by the black rectangle at the centre of the circle.

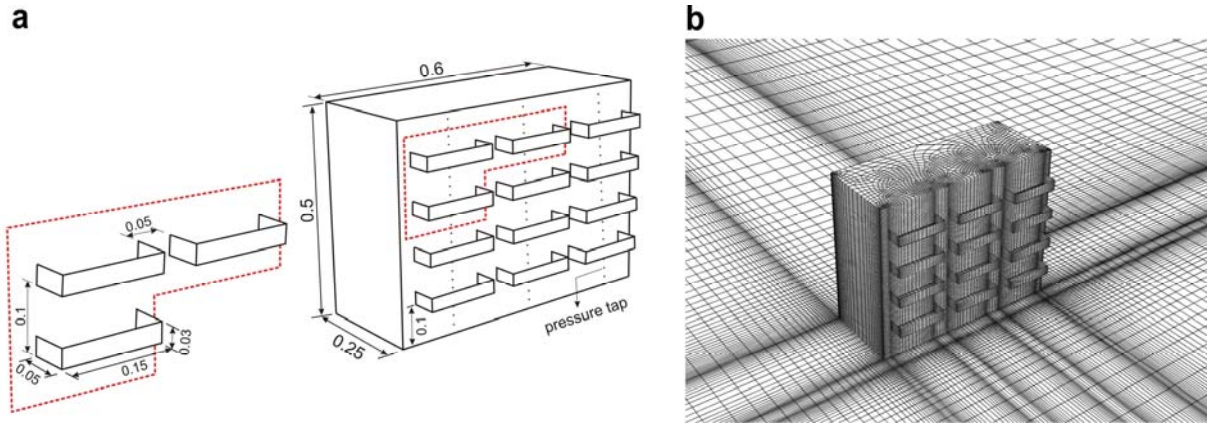

Figure 5. (a) Wind-tunnel model of building with balconies for CFD validation and three vertical lines for pressure measurements (reduced-scale dimensions in m); (b) Computational grid at building surfaces and ground surface (2,102,250 cells).

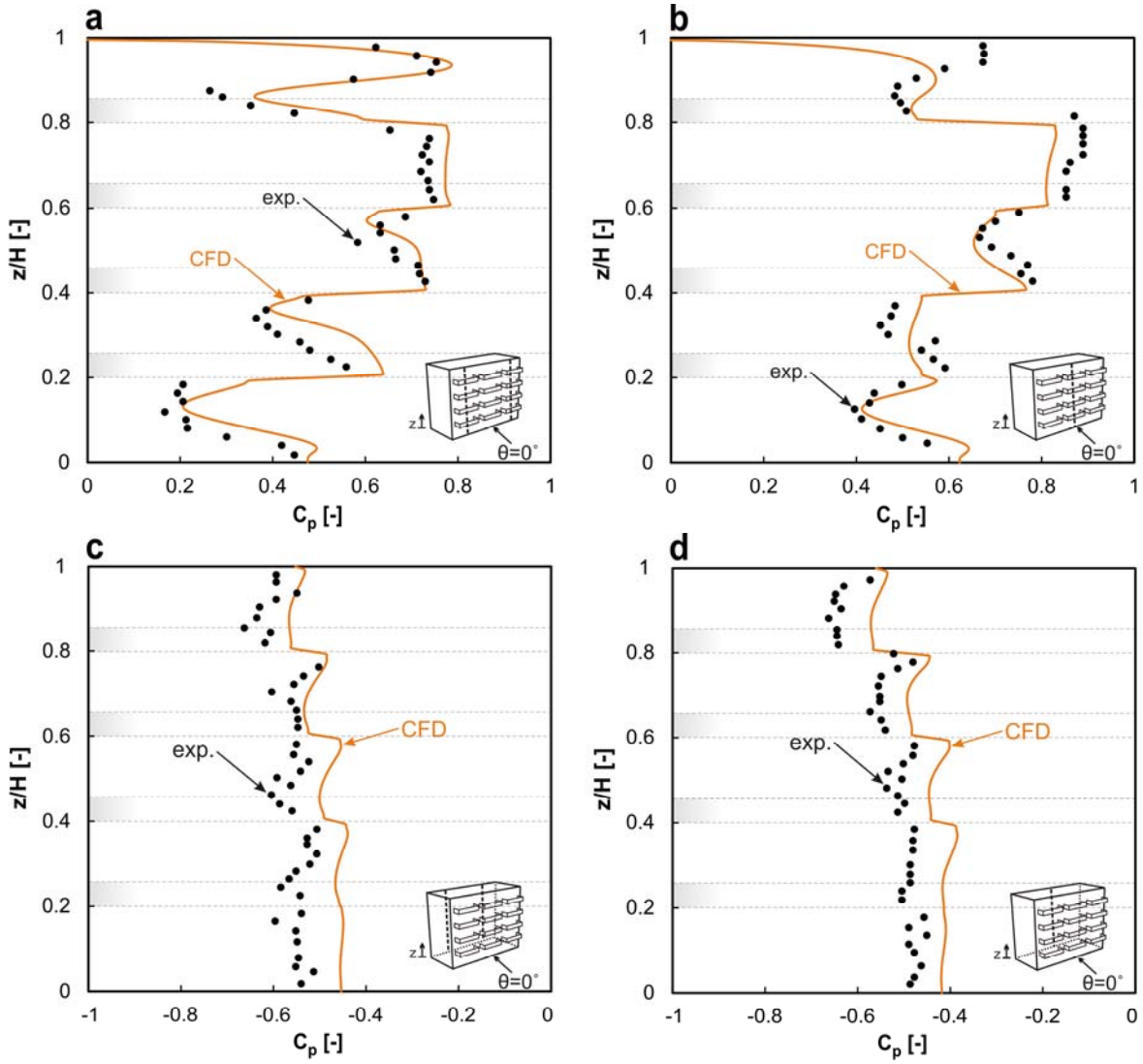

Figure 6. CFD validation: comparison of simulated and measured pressure coefficient (C_P) for perpendicular wind direction (0º) along: (a) windward edge lines; (b) windward centre line; (c) leeward edge lines; (d) leeward centre line.

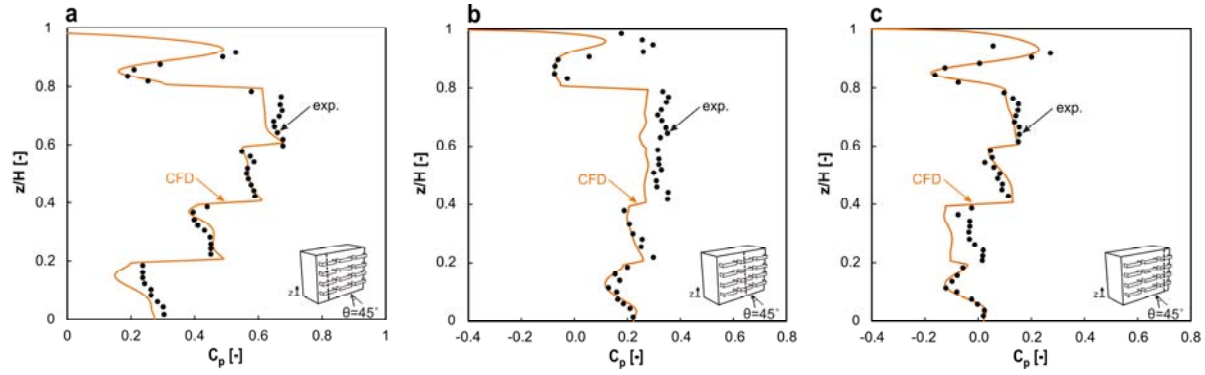

Figure 7. CFD validation: comparison of simulated and measured pressure coefficient (C_P) for oblique wind direction (45º) along: (a) windward upstream edge line; (b) windward centre line; (c) windward downstream edge line.

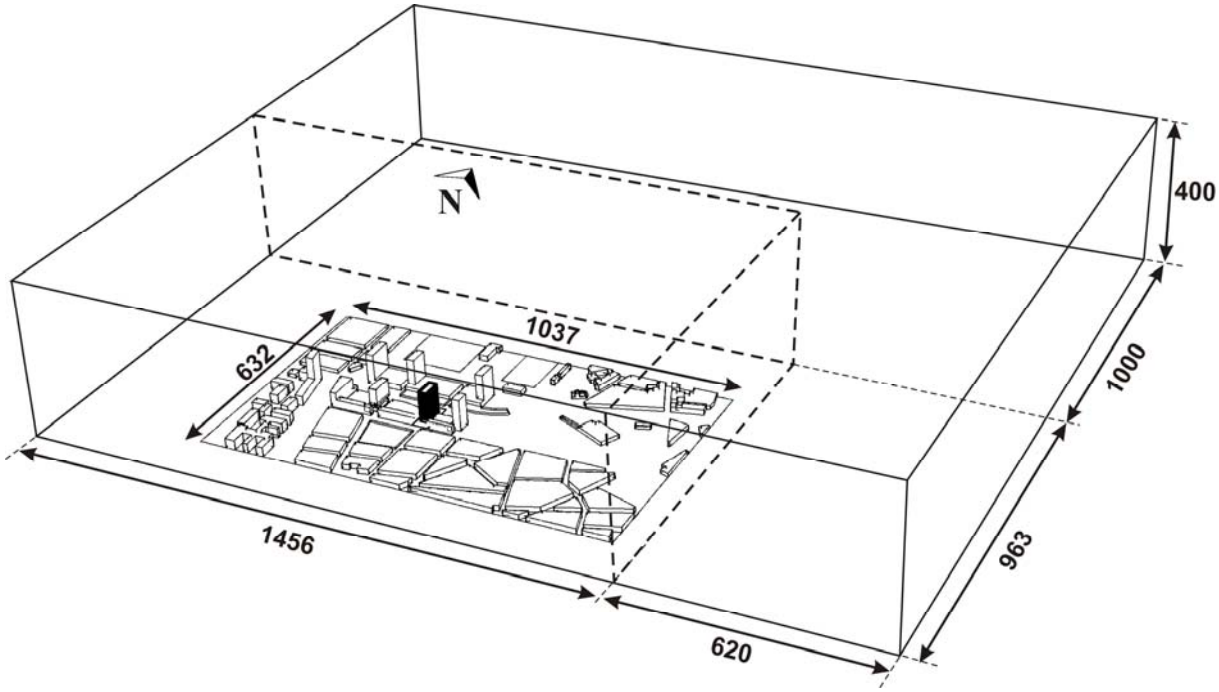

Figure 8. Computational domain for wind directions 180° to 270°, consisting of a basic domain and an additional downstream domain. Dimensions in meter.

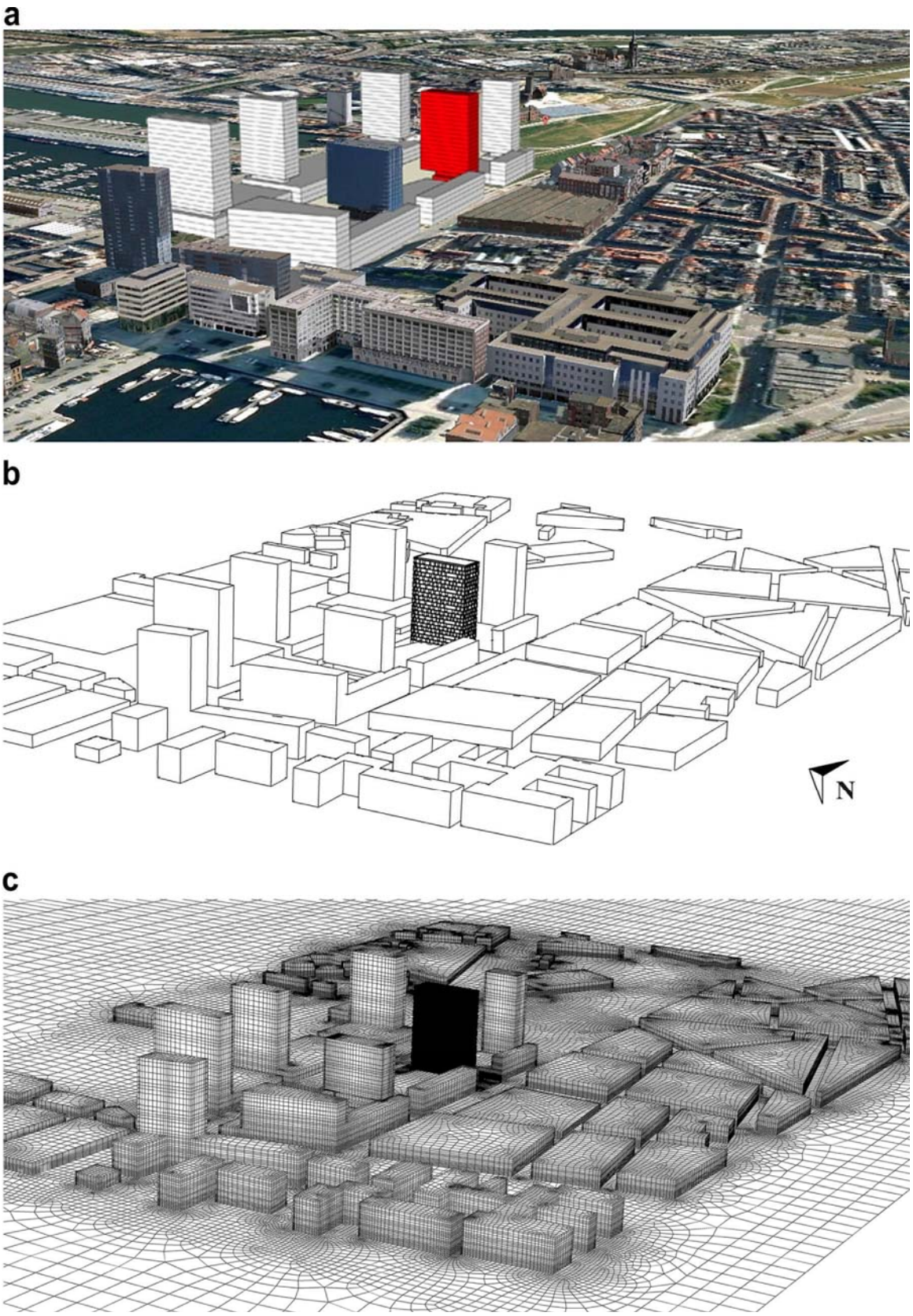

Figure 9. (a) Aerial view of the Park Tower (red) and surrounding buildings. (b) Corresponding computational geometry and (c) high-resolution computational grid (16,292,495 cells).

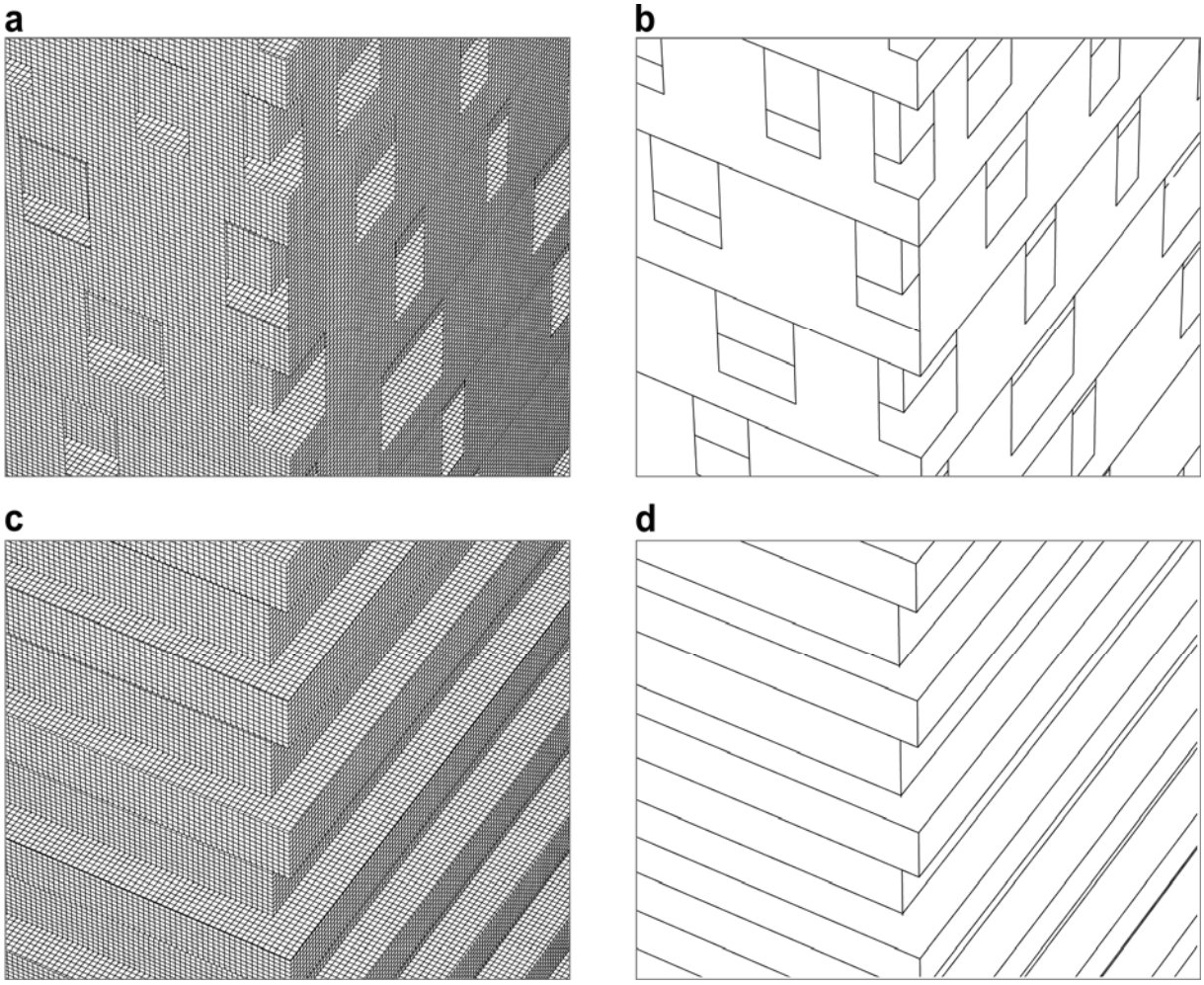

Figure 10. Detail of computational grid near the south-west corner of the 15th floor for the case (a,b) with second-skin facade concept (16,292,495 cells) and (c,d) without this concept (15,536,529 cells).

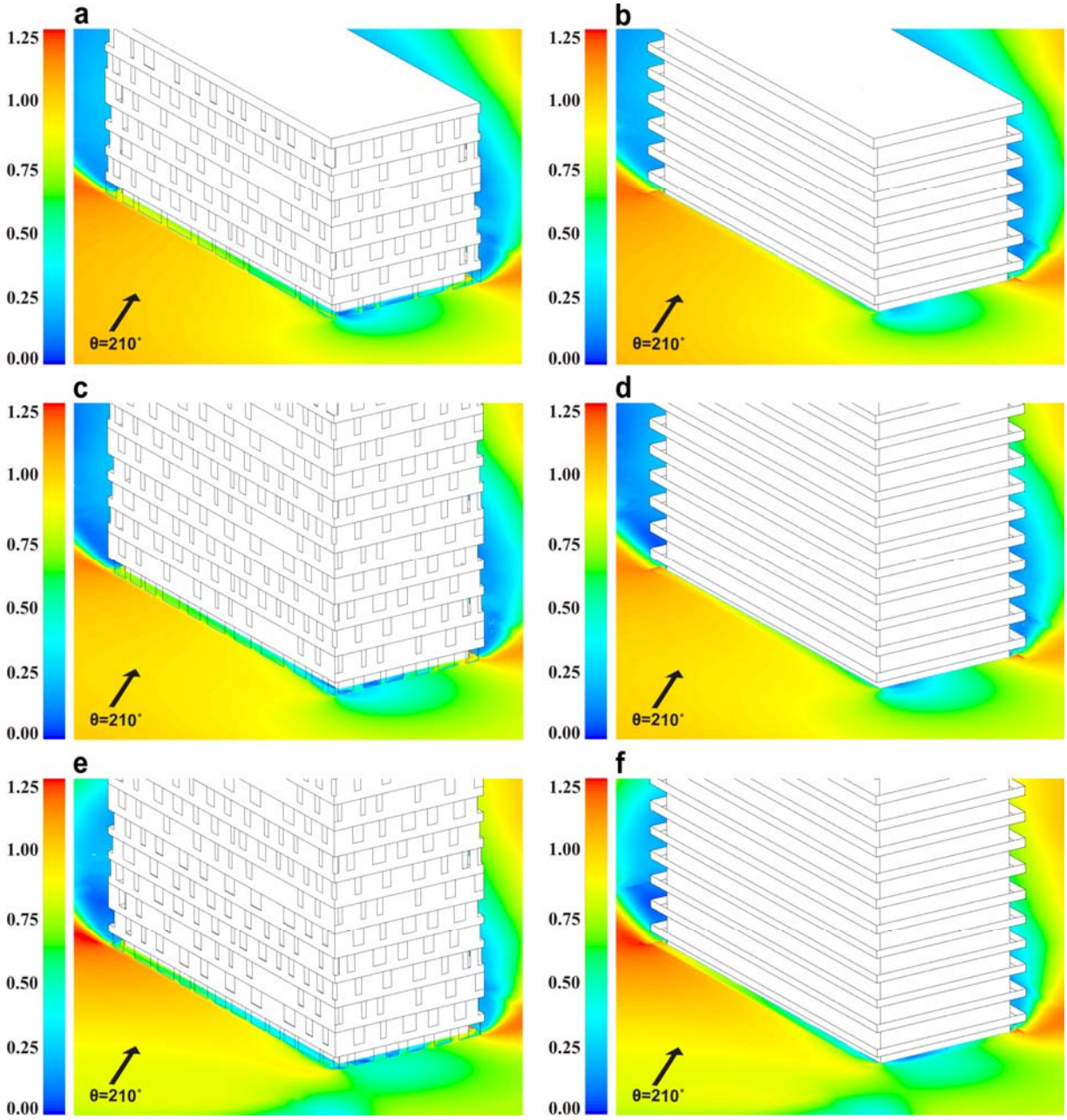

Figure 11. Perspective view of contours of amplification factor in a horizontal plane at a height of 1.7 m above floor level for wind direction 210°: (a,c,e) 15th, 10th and 5th floor of the tower with second-skin facade concept; (b,d,f) same for case without this concept.

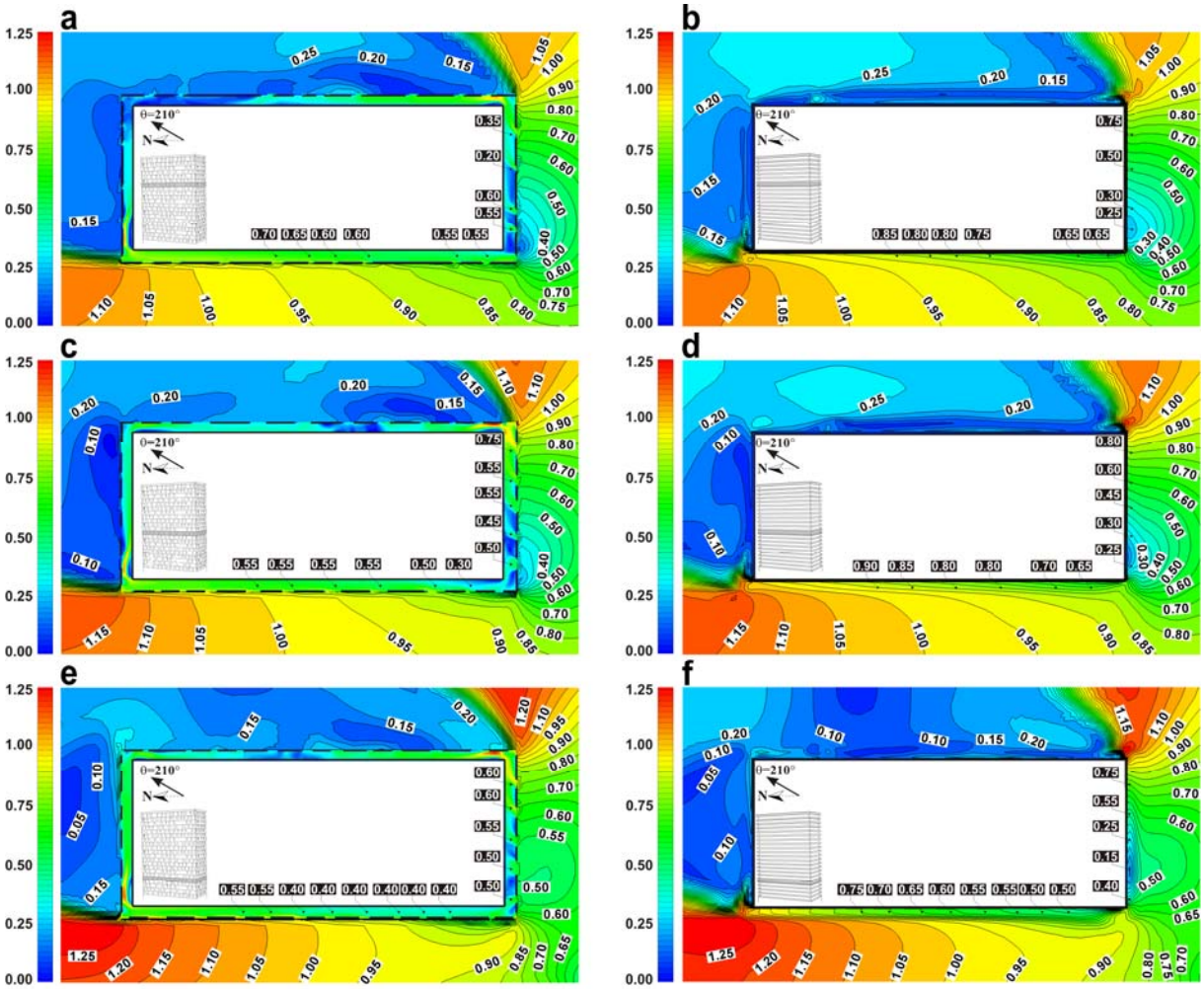

Figure 12. Top view of contours of amplification factor in a horizontal plane at a height of 1.7 m above balcony level for wind direction 210°: (a,c,e) 15th, 10th and 5th floor of the tower with second-skin facade concept; (b,d,f) Same for case without this concept.

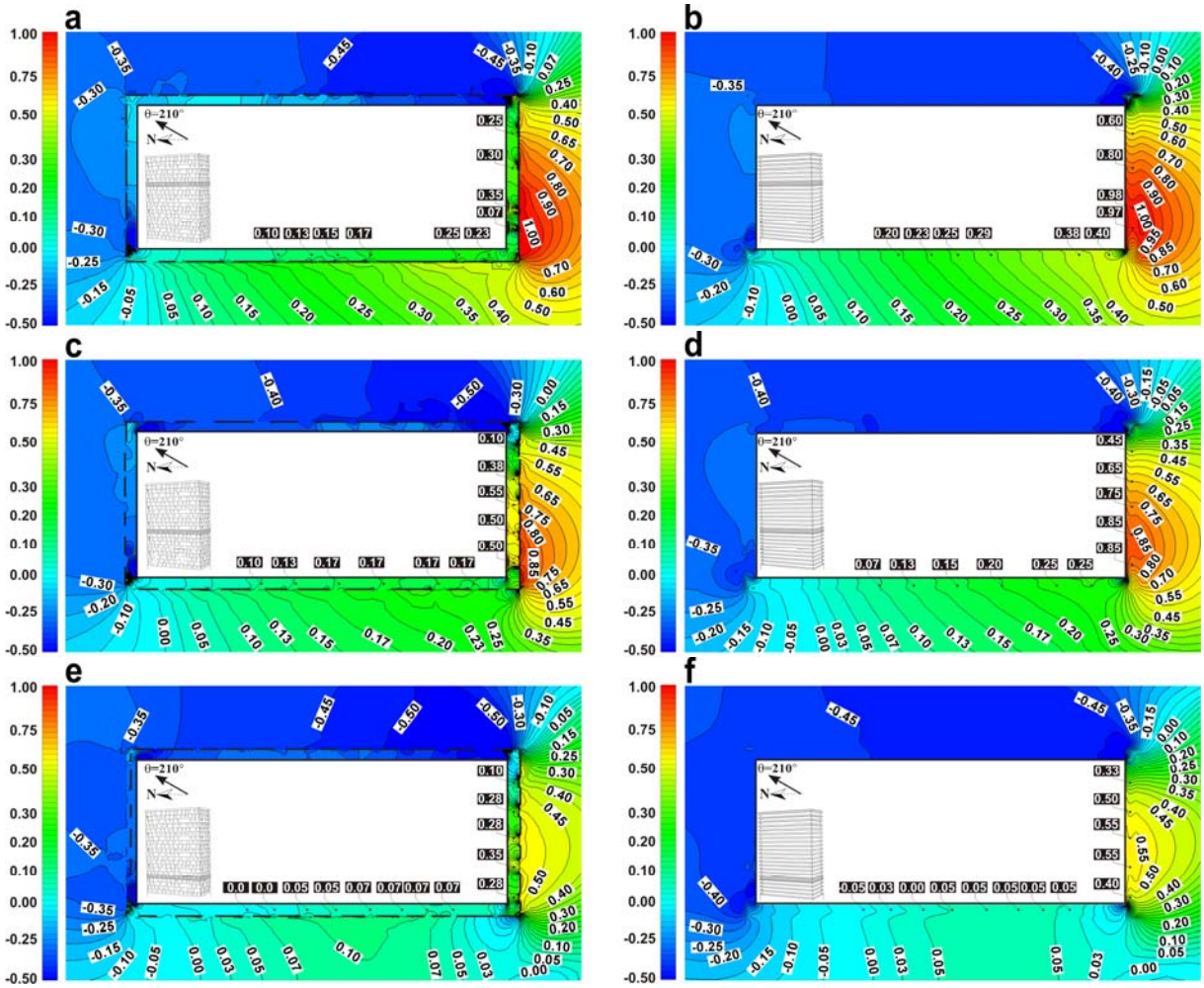

Figure 13. Top view of contours of static pressure coefficient in a horizontal plane at a height of 1.7 m above balcony level for wind direction 210°: (a,c,e) 15th, 10th and 5th floor of the tower with second-skin facade concept; (b,d,f) Same for case without this concept.

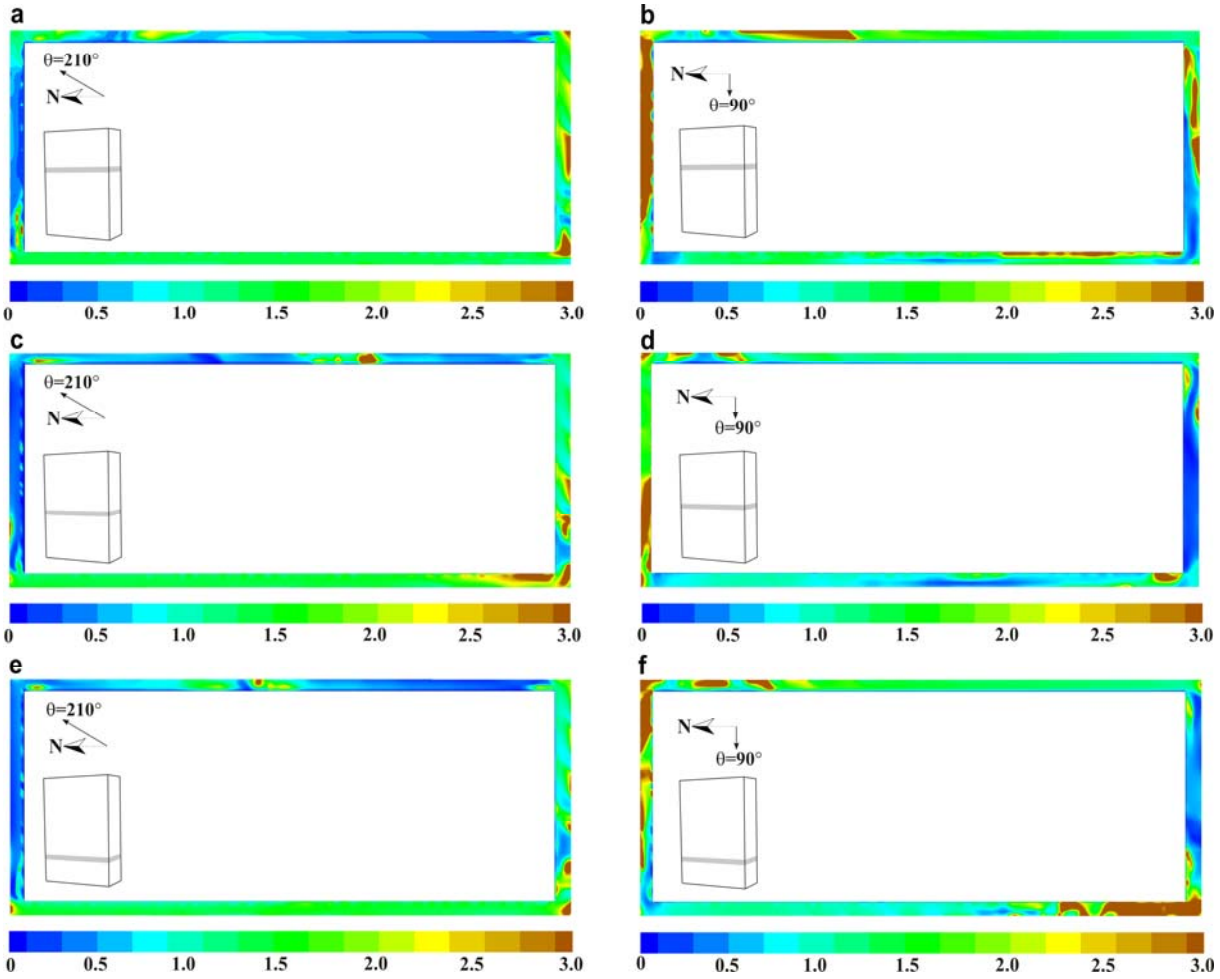

Figure 14. Top view of contours of ratio of mean wind speed without second-skin facade concept and mean wind speed with this concept, in a horizontal plane at a height of 1.7 m above balcony level for wind directions 210° and 90°, and for three floors: 15th, 10th and 5th floor.

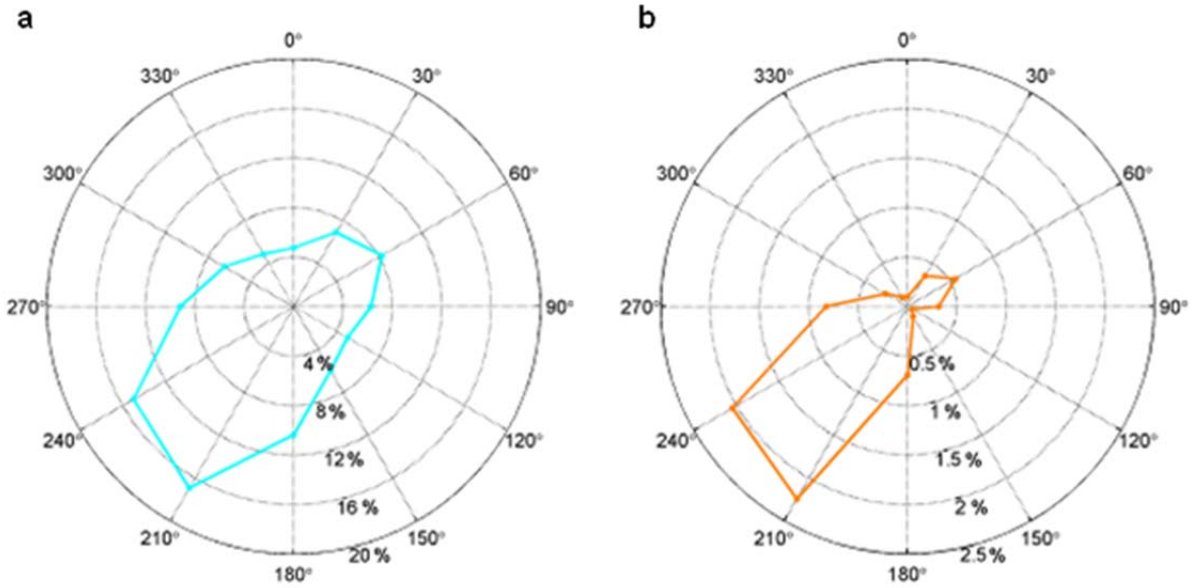

Figure 15. Wind roses for Eindhoven meteorological station to be used for Antwerp. (a) Standard wind rose with frequency distribution of the hourly mean wind speed. (b) Wind rose with exceedance probability of the 5 m/s threshold at pedestrian height of 1.7 m, based on virtual open field conditions with z_0 = 0.03 m.

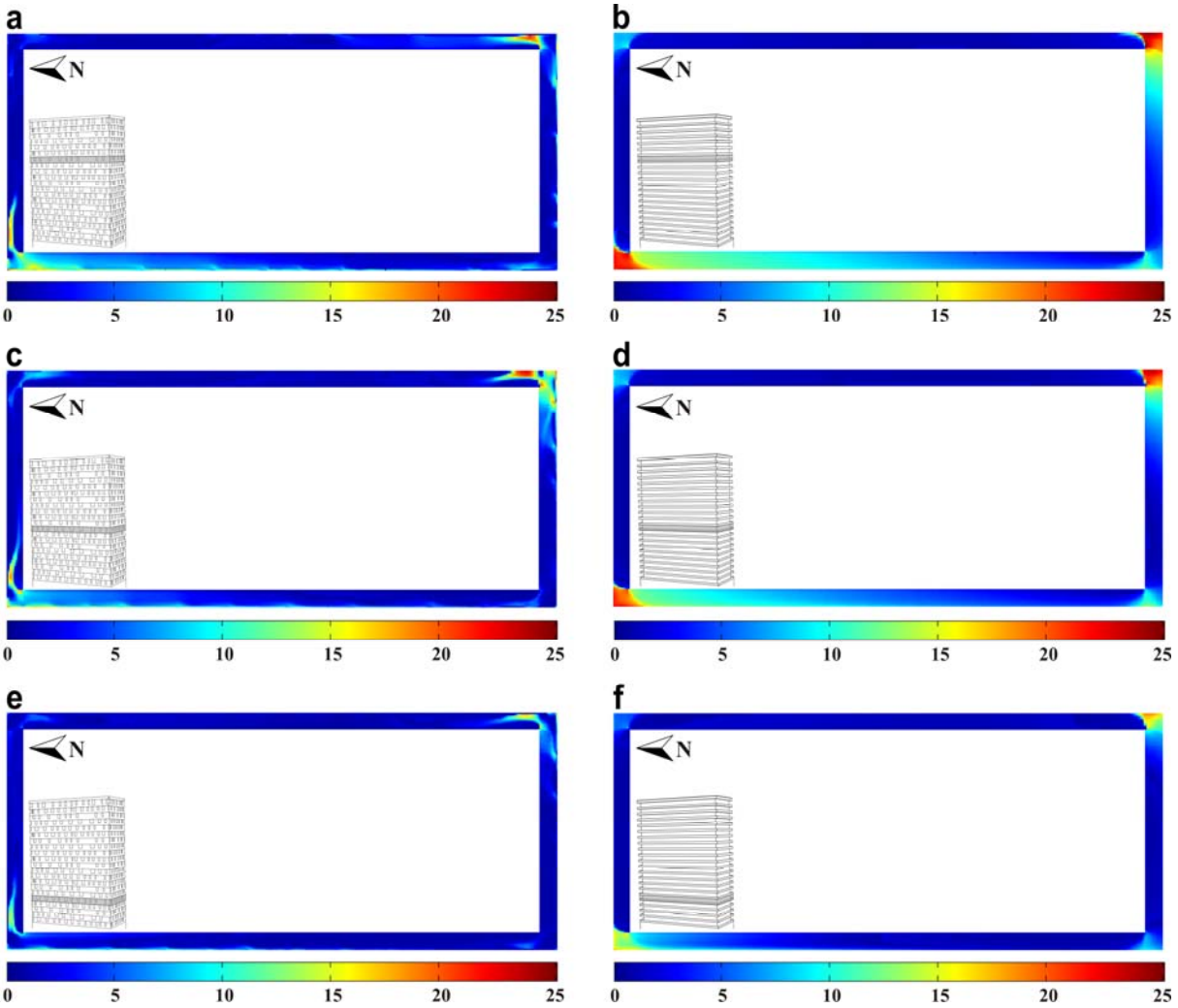

Figure 16. Top view of contours of exceedance probability for wind nuisance in a horizontal plane at a height of 1.7 m above balcony level: (a,c,e) 15th, 10th and 5th floor of the tower with second-skin facade concept; (b,d,f) same for case without this concept.

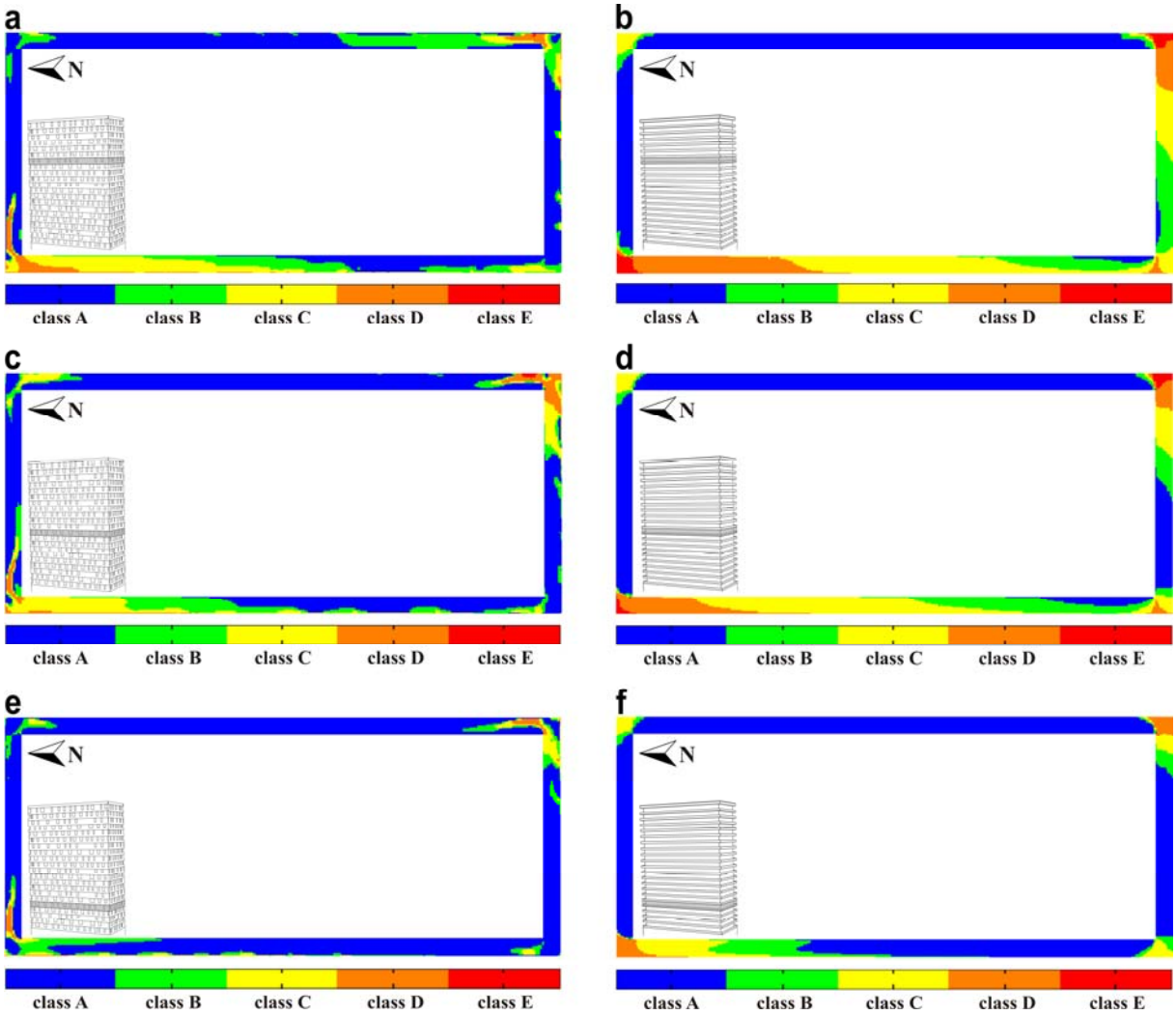

Figure 17. Top view of contours of wind comfort quality classes according to NEN8100 in a horizontal plane at a height of 1.7 m above balcony level: (a,c,e) 15th, 10th and 5th floor of the tower with second-skin facade concept; (b,d,f) Same for case without this concept.

TABLES

Table 1. Criteria for wind comfort according to NEN 8100 [12].

$P(U_{THR} > 5$ m/s) (in % hours per year)	Quality Class	Activity		
		Traversing	Strolling	Sitting
< 2.5	A	Good	Good	Good
2.5 – 5.0	B	Good	Good	Moderate
5.0 – 10	C	Good	Moderate	Poor
10 – 20	D	Moderate	Poor	Poor
> 20	E	Poor	Poor	Poor